

****FULL TITLE****
*ASP Conference Series, Vol. **VOLUME**, **YEAR OF PUBLICATION***
****NAMES OF EDITORS****

Evolution of massive black hole spins

Marta Volonteri

*Department of Astronomy, University of Michigan, Ann Arbor, MI,
 48109, USA*

Abstract. Black hole spins affect the efficiency of the “classical” accretion processes, hence the radiative output from quasars. Spins also determine how much energy is extractable from the hole itself. Recently it became clear that massive black hole spins also affect the retention of black holes in galaxy, because of the impulsive “gravitational recoil”, up to thousands km/s, due to anisotropic emission of gravitational waves at merger. I discuss here the evolution of massive black hole spins along the cosmic history, due to the combination of mergers and accretion events. I describe recent simulations of accreting black holes in merger remnants, and discuss the implication for the spins of black holes in quasars.

1. Introduction

Black holes, as physical entities, span the full range of masses, from tiny black holes predicted by string theory, to monsters weighing by themselves almost as much as a dwarf galaxy (MBHs). Notwithstanding the several orders of magnitude difference between the smallest and the largest black hole known, all of them can be described by only three parameters: mass, spin and charge. Astrophysical black holes are even simpler, as charge can be neglected. So, besides their masses, M_{BH} , astrophysical black holes are completely characterized by their dimensionless spin parameter, $a \equiv J_h/J_{\text{max}} = c J_h/G M_{\text{BH}}^2$, where J_h is the angular momentum of the black hole, and $0 \leq a \leq 1$.

1.1. Radiative efficiency

In radiatively efficient, geometrically thin accretion disks the mass-to-energy conversion efficiency, ϵ , equals $\epsilon \equiv 1 - E/M_{\text{BH}}c^2$, where E is the binding energy per unit mass of a particle in the innermost stable circular orbit (ISCO). The location of the ISCO depends solely on a black hole spin, shrinking by a factor of 6 between a non-rotating hole and its maximally rotating counterpart¹. The closer the ISCO is to the horizon, the higher the mass-to-energy conversion efficiency, which increases from 6% to 42% in the above example. The mass-to-energy

¹We will use the term “maximally rotating” for a black hole with $a = 1$, although we note that Thorne (1974) showed that accretion driven spin-up is limited to $a = 0.998$. Magnetic fields connecting material in the disk and the plunging region may further reduce the equilibrium spin. Magnetohydrodynamic simulations for a series of thick accretion disks suggest an asymptotic equilibrium spin at $a \approx 0.9$ (Gammie et al. 2004). The location of the ISCO depends also on the particle being on a prograde or retrograde orbit. The ISCO for a particle on a retrograde orbit around a hole with $a = 1$ is 9 times larger than for its prograde counterpart.

conversion directly affects the mass-growth rate of black holes: high efficiency implies slow growth. More precisely, for a hole accreting at the Eddington rate, the black hole mass increases with time as:

$$M(t) = M(0) \exp\left(\frac{1 - \epsilon}{\epsilon} \frac{t}{t_{\text{Edd}}}\right), \quad (1)$$

where $t_{\text{Edd}} = 0.45 \text{ Gyr}$. The higher the spin, the higher ϵ , implying longer timescales to grow the MBH mass by the same number of e-foldings. Going from $\epsilon = 0.06$ to $\epsilon = 0.42$, the difference in $M(t)$ amounts to 6 orders of magnitude, at $t = t_{\text{Edd}}$. The typical spin therefore affects the overall mass-growth of MBHs, and the duty cycle of quasars.

The radiative efficiency is also the fundamental free parameter for the Soltan argument (Soltan 1982) and, more recently, synthesis models (e.g., Merloni & Heinz 2008) which relate the integrated MBH mass density to the integrated emissivity of the AGN population, via the integral of the luminosity function of quasars. If the average efficiency of converting accreted mass into luminosity is $\epsilon = L/\dot{M}c^2$, then the MBH will increase its mass by $\dot{M}_{\text{BH}} = (1 - \epsilon)\dot{M}$, accounting for the fraction of the incoming mass that is radiated away. Applying this argument to the whole MBH population, the MBH mass density can be related to the integral of the LF of quasar, $\Psi(L, z)$, with *the radiative efficiency being a free parameter*.

1.2. Relativistic jets

The so-called “spin paradigm” asserts that powerful relativistic jets are produced in AGNs with fast rotating black holes (Blandford et al. 1990), implying that MBHs rotate slowly in radio-quiet quasars, which represent the majority of quasars (Wilson & Colbert 1995). However, if we expect the same mathematical and physical properties to describe both the black holes of a few solar masses and MBHs, such conjecture, at least in its basic interpretation, is at odds with studies of radio-emission from X-ray binaries (e.g., Ulvestad & Ho 2001; K rding et al. 2006). These works showed that the production of jets is intermittent, although the spin of stellar mass black holes is not expected to vary over the same timescales. *Why and when* jet form, and what is the role of spin (if any) in jet production has not been explained yet.

1.3. Gravitational recoil

MBH spins affect the frequency of MBHs in galaxies, via the “gravitational recoil” mechanism. When the members of a black hole binary coalesce, the center of mass of the coalescing system recoils due to the non-zero net linear momentum carried away by gravitational waves in the coalescence. If this recoil were sufficiently violent, the merged hole would break loose from the host and leave an empty nest. Recent breakthroughs in numerical relativity have allowed reliable computations of black hole mergers and recoil velocities, taking the effects of spin into account. Non-spinning MBHs, or binaries where MBH spins are *aligned* with the orbital angular momentum are expected to recoil with velocities below 200 km s^{-1} . The recoil is much larger, up to thousands km s^{-1} , for MBHs with large spins in non-aligned configurations (Campanelli et al. 2007; Gonz lez et al. 2007; Herrmann et al. 2007).

2. Cosmic evolution of MBH spins

MBH spins determine directly the radiative efficiency of quasars. On the other hand, accretion determines MBH spins. A hole that is initially non-rotating gets spun up to a maximally-rotating state ($a = 1$) after increasing its mass by a factor $\sqrt{6} \simeq 2.4$. A maximally-rotating hole is spun down by retrograde accretion to $a = 0$ after growing by a factor $\sqrt{3/2} \simeq 1.22$. A 180° flip of the spin of an extreme-Kerr hole will occur after tripling its mass. Spin-up is therefore a natural consequence of prolonged disk-mode accretion: any hole that increases substantially its mass by capturing material with constant angular momentum axis would end up spinning rapidly (“coherent accretion”). If the lifetime of quasars is long enough that angular momentum coupling between black holes and accretion discs through the Bardeen-Petterson effect effectively forces the innermost region of accretion discs to align, then quasar MBHs should have large spins Volonteri et al. (2005). Spin-down occurs when counter-rotating material is accreted, if the angular momentum of the accretion disk is strongly misaligned with respect to the direction of the MBH spin. If accretion proceeds via small (and short) uncorrelated episodes (“chaotic accretion”, King & Pringle 2006), where accretion of co-rotating and counter-rotating material is equally probable, then spins tend to be low. This is because counter-rotating material spins MBHs down more efficiently than co-rotating material spins them up (as the ISCO for a retrograde orbit is at larger radii than for a prograde orbit, the transfer of angular momentum is more efficient in the former case.)

MBH-MBH mergers also influence the spin evolution. Berti & Volonteri (2008) consider how the dynamics of BH mergers influences the final spin. Except in the case of aligned mergers, a sequence of BH mergers can lead to large spins > 0.9 *only if* MBHs start already with large spins *and* they do not experience many major mergers. Therefore, the common assumption that mergers between MBHs of similar mass always lead to large spins needs to be revised.

3. Spin evolution in gas-rich merger remnants

Gas-rich mergers between galaxies of comparable mass (i.e. major mergers), are advocated to drive quasar activity, hence MBH growth. The evolution of MBH spins has to be addressed by simulating the typical environmental conditions expected around quasars, where the properties of the accretion flow are established. When accretion is triggered by galaxy mergers, as expected for quasars, the material that will feed MBHs is expected to assemble into a circumnuclear disk. These disks may be the end-product of gas-dynamical, gravitational torques excited during the merger, when large amounts of gas are driven into the core of the remnant (Mayer et al. 2007). This last phase of the merger has been suggested to be associated to quasar activity. These are therefore the most relevant circumstances to be explored. During their inspiral MBHs are surrounded by a dense cocoon of gas that drives their dynamical decay and provides fuel for the feeding of the holes (Dotti et al. 2006, 2007). Since matter carries angular momentum also the spin vector can change during the accretion process. The details of the dynamics may have a profound influence on the mass and spin evolution of the two MBHs.

3.1. Simulation set-up

Dotti et al. (2010) follow the dynamics of MBH pairs in nuclear discs using numerical simulations run with the N-Body/SPH code GADGET (Springel, Yoshida & White 2001), upgraded to include the accretion physics (Dotti et al. 2009). In our models, two MBHs are placed in the plane of a massive circumnuclear gaseous disc, embedded in a larger stellar spheroid. The disc is modeled with 2×10^6 particles, has a total mass $10^8 M_\odot$, and follows a Mestel surface density profile. The spatial resolution of the hydrodynamical force is ≈ 0.1 pc. With this spatial resolution the Bondi radius of the holes is resolved. The disc is rotationally supported and Toomre stable. SPH disk particles evolve with a purely adiabatic equation of state, described by either a polytropic index $\gamma = 7/5$ that mimics a star-forming region (“cold” disk, Spaans & Silk 2000), or $\gamma = 5/3$ that includes extra heat, e.g, AGN feedback (“hot” disk; see, e.g. Mayer et al. 2007).

The spheroidal component (bulge) is modeled with 10^5 collisionless particles, initially distributed as a Plummer sphere with a total mass $\simeq 7 \times$ the disc mass. The mass of the bulge within 100 pc is five times the mass of the disc (Downes & Solomon 1998). The two MBHs (M_1 and M_2) are equal in mass ($M_{\text{BH}} = 4 \times 10^6 M_\odot$). M_1 , called primary for reference, is placed at rest at the centre of the circumnuclear disc. M_2 , termed secondary, is moving on an initially eccentric ($e_0 \simeq 0.7$) counterrotating (retrograde MBH) or corotating (prograde MBH) orbit with respect to the circumnuclear disc. Gas particles are accreted onto a MBH if they lie within its Bondi radius, and if the total mass accreted onto a MBH in a timestep is lower than \dot{M}_{Edd} . We find accretion rates close to Eddington for the central MBH (M_1) is in good agreement with the suggestion that quasars shine during the last phases of galaxy mergers. The secondary MBH in the simulation (M_2) accretes instead at sub-Eddington rates during most of its orbital decay.

Each gas particle accreted by the MBH carries with it angular momentum. From the properties of the accreted particles we can compute, as a function of time, the mass accretion rate and the versor $\hat{\mathbf{l}}_{\text{edge}}$, that defines the direction of the total angular momentum of the accreted particles. This information can be gathered only by performing very high resolution simulations. In our runs, the spatial resolution of the hydrodynamical force in the highest density regions is ≈ 0.1 pc, well below the Bondi radius.

3.2. Modelling the evolution of spin vectors

We use the MBH accretion histories obtained from our SPH simulations to follow the evolution of each MBH spin vector, $\mathbf{J}_{\text{BH}} = (aGM_{\text{BH}}^2/c)\hat{\mathbf{J}}_{\text{BH}}$, where $0 \leq a \leq 1$ is the adimensional spin parameter and $\hat{\mathbf{J}}_{\text{BH}}$ is the spin versor. The scheme we adopt to study the spin evolution is based on the model recently developed by Perego et al. (2009). Here we summarize the algorithm used.

We assume that during any accretion event recorded in our SPH simulations, the inflowing gas forms a geometrically thin/optically thick α -disc (Shakura & Sunyaev 1973) on milli-parsec scales (not resolved in the simulation), and that the outer disc orientation is defined by the unit vector \mathbf{l}_{edge} . The evolution of the α -disc is related to the radial viscosity ν_1 and the vertical viscosity ν_2 : ν_1 is the

standard radial shear viscosity while ν_2 is the vertical shear viscosity associated to the diffusion of vertical warps through the disc. The two viscosities can be described in terms of two different dimensionless viscosity parameters, α_1 and α_2 , through the relations $\nu_{1,2} = \alpha_{1,2} H c_s$, where H is the disc vertical scale height and c_s is the sound speed of the gas in the accretion disc. We further assume $\alpha_2 = f_2/(2\alpha_1)$, with $\alpha_1 = 0.1$ and $f_2 = 0.6$ (Lodato & Pringle 2007). We assume power law profiles for the two viscosities, $\nu_{1,2} \propto R^{3/4}$, as in the Shakura & Sunyaev solution.

As shown by Bardeen & Petterson (1975), if the orbital angular momentum of the disc around the MBH is misaligned with respect to the MBH spin, the coupled action of viscosity and relativistic Lense-Thirring precession warps the disc in its innermost region forcing the fluid to rotate in the equatorial plane of the spinning MBH. The timescale of propagation of the warp is short compared with the viscous/accretion timescale so that the deformed disc reaches an equilibrium profile that can be computed by solving for the equation

$$\frac{1}{R} \frac{\partial}{\partial R} (R L v_R) = \frac{1}{R} \frac{\partial}{\partial R} \left(\nu_1 \Sigma R^3 \frac{d\Omega}{dR} \hat{\mathbf{i}} \right) + \frac{1}{R} \frac{\partial}{\partial R} \left(\frac{1}{2} \nu_2 R L \frac{\partial \hat{\mathbf{i}}}{\partial R} \right) + \frac{2G \mathbf{J}_{\text{BH}} \times \mathbf{L}}{c^2 R^3} \quad (2)$$

where v_R is the radial drift velocity, Σ is the surface density, and Ω is the Keplerian velocity of the gas in the disc. \mathbf{L} is the local angular momentum surface density of the disc, defined by its modulus L and the versor $\hat{\mathbf{i}}$ that define its direction.

The boundary conditions to eq. 2 are the direction of \mathbf{L} at the outer edge $\hat{\mathbf{i}}_{\text{edge}}$, the mass accretion rate (that fixes the magnitude of Σ), and the values of mass and spin of each MBH. All these values but the MBH spins are directly obtained from the SPH runs. In particular, the direction of the unit vector $\hat{\mathbf{i}}_{\text{edge}}$ is computed considering those SPH particles nearing the MBH gravitational sphere of influence that are accreted according to the criteria outlined above.

The MBH spin changes also in response to its gravito-magnetic interaction with the disc on a timescale longer than the time scale of warp propagation (Perego et al. 2009). This interaction tends to reduce the degree of misalignment between the disc and the spin decreasing with time the angle between \mathbf{J}_{BH} and $\hat{\mathbf{i}}_{\text{edge}}$. The MBH spin evolution is followed by solving the following equation:

$$\frac{d\mathbf{J}_{\text{BH}}}{dt} = \dot{M} \Lambda(R_{\text{ISO}}) \hat{\mathbf{i}}(R_{\text{ISO}}) + \frac{4\pi G}{c^2} \int_{\text{disc}} \frac{\mathbf{L} \times \mathbf{J}_{\text{BH}}}{R^2} dR. \quad (3)$$

The first term in eq. 3 accounts for the angular momentum deposited onto the MBH by the accreted particles at the innermost stable orbit (ISO), where $\Lambda(R_{\text{ISO}})$ denotes the specific angular momentum at R_{ISO} and $\hat{\mathbf{i}}(R_{\text{ISO}})$ the unit vector parallel to \mathbf{J}_{BH} , describing the warped disc according to the Bardeen-Petterson effect. The second term instead accounts for the gravo-magnetic interaction of the MBH spin with the warped disc. It modifies only the MBH spin direction (and not its modulus), conserving the total angular momentum of the composite (MBH+disc) system (King et al. 2005). We applied iteratively eq. 1 and 2 using inputs from the SPH simulation that give the values of the mass accretion rate, the MBH mass and the direction of $\hat{\mathbf{i}}_{\text{edge}}$. The algorithm

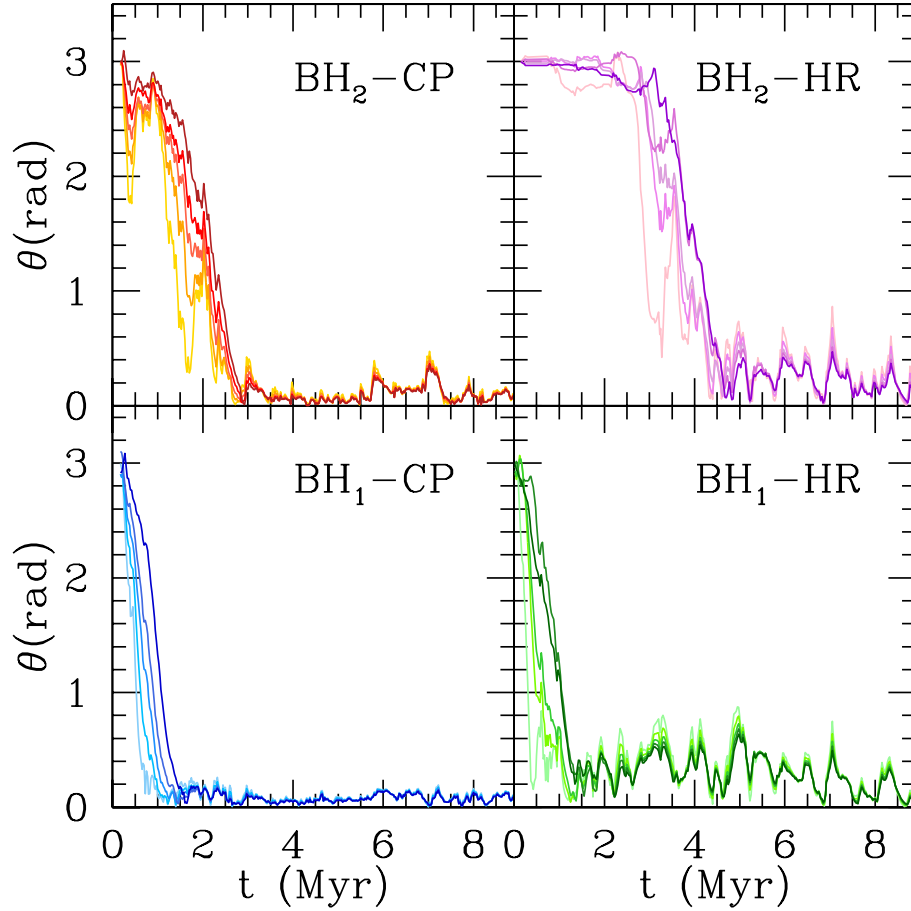


Figure 1. Upper panels: time evolution of the relative angle between M_2 (secondary MBH) spin and the orbital angular momentum of the MBH pair. Left (right) panel refers to a “cold” (“hot”) disk. The initial angle is arbitrarily set to 2.5 radians (close to anti-aligned), and the initial spin parameter magnitudes varies between 0.2 (lighter colours) to 1 (darker colours). Lower panels: same as upper panels for M_1 (primary MBH).

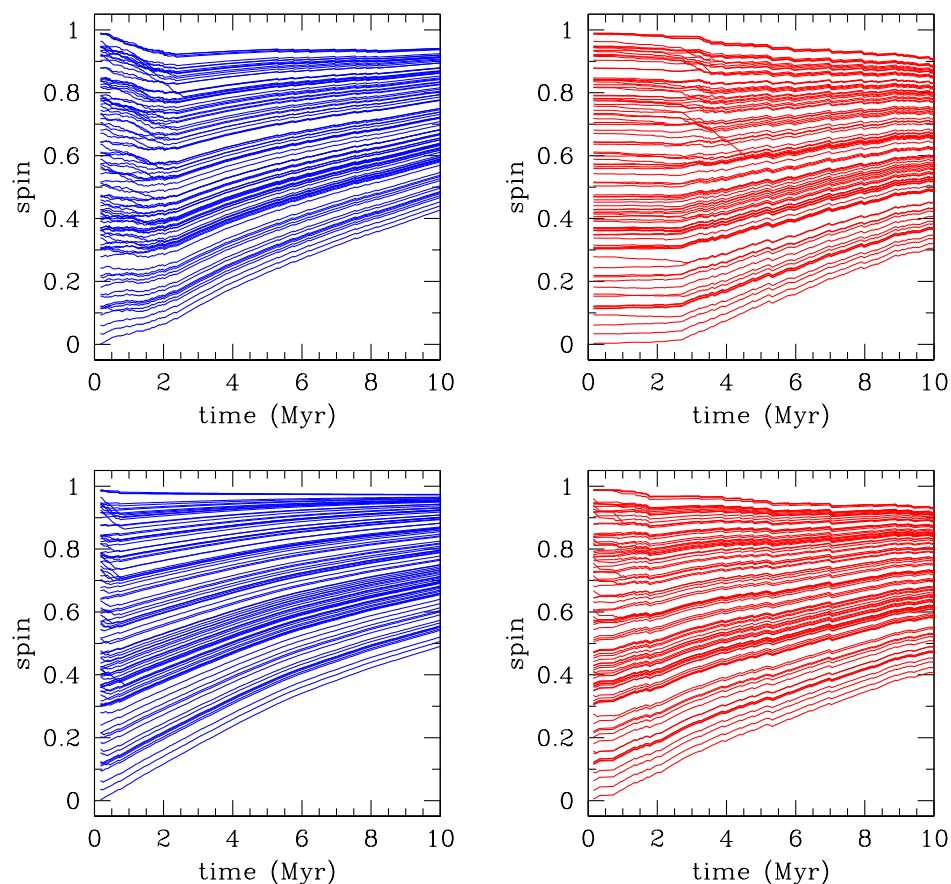


Figure 2. Left: spin evolution for MBHs embedded in a “cold” circumnuclear disk. In a “cold” disk, where turbulence and pressure are relatively unimportant, most of the accreted material has angular momentum directed along the same axis, leading to mostly “coherent” accretion. Right: same quantities, but for a MBH evolving in a more chaotic “hot” circumnuclear disk. Here the direction of the angular momentum of the accreted gas is much more variable, giving rise to a “chaotic” flow, and the magnitude of the MBH spins ends up being lower, at a given time along the simulation. Bottom: primary, central, MBH. Top: secondary MBH. In each panel we show 100 realizations starting from a flat distribution in spin magnitudes and initial orientations.

returns, as output, the spin vector, that is, its magnitude and direction. At each timestep our code therefore provides the angle between the spin vector of each MBH and the angular momentum vector of their relative orbit.

3.3. Spins: alignment and magnitudes

Figure 1 shows the time evolution of the relative angle θ between the spin of each MBH and the orbital angular momentum of the MBH pair. The initial relative angle has been arbitrarily set to 2.5 radians (143°), while a has initially five different values (0.2, 0.4, 0.6, 0.8, and 1). In all cases we find that MBH spins lose memory of their initial orientation: accretion torques suffice to align the spins with the angular momentum of their orbit on a short timescale ($\lesssim 1 - 2$ Myr). A residual off-set in the spin direction relative to the orbital angular momentum remains, at the level of $\lesssim 10^\circ$ for the case of a cold disc, and $\lesssim 30^\circ$ for a warmer disc. Alignment in a cooler disc is more effective due to the higher coherence of the accretion flow near each MBH that reflects the large-scale coherence of the disc’s rotation. If the MBHs coalesce preserving the spin directions set after formation of a Keplerian binary, the MBH resulting from their coalescence receives a relative small kick, $\lesssim 100 \text{ km s}^{-1}$.

Fig. 2 shows the time evolution of the spin magnitudes (Dotti et al. in preparation). We show here 100 realizations starting from a flat distribution in spin magnitudes and initial orientations. We find that initially maximally rotating holes are spun down, and initially slowly rotating holes are spun up, leading to intermediate equilibrium values ($\simeq 0.6 - 0.8$). The spin of the secondary MBH tends to be slightly lower, because of a higher incidence of counterrotating events. It is suggestive that measured spins cluster around these values. The best measurement to date is the Seyfert galaxy MCG-6-30-15. In this Seyfert, the iron line is so broad as to rigorously require $a = 0.9 \pm 0.1$ (Brenneman & Reynolds 2006). Miniutti et al. (2009) reported a spin parameter of $a = 0.6 \pm 0.2$ in the narrow-line Seyfert-1 AGN SWIFT J2127.4+5654. The X-ray spectrum of Fairall 9 also results in a spin $a = 0.7 \pm 0.2$ at 99% confidence (Schmoll et al. 2009).

4. MBH spins and galaxy morphology

If the events powering quasars coincide with the formation of elliptical galaxies (di Matteo et al. 2005), we might expect that the MBH hosted by an elliptical galaxy had, as last major accretion episode, a large increase in its mass. During this episode the spin increased significantly as well, possibly up to very high values, $a \simeq 0.6 - 0.8$, as suggested in the previous section.

Black holes in spiral galaxies, on the other hand, probably had their last major merger (i.e., last major accretion episode), if any, at high redshift, so that enough time elapsed for the galaxy disc to reform. Moreover, several observations suggest that single accretion events last $\simeq 10^5$ years in Seyfert galaxies, while the total activity lifetime (based on the fraction of disc galaxies that are Seyfert) is $10^8 - 10^9$ years (e.g., Kharb et al. 2006; Ho et al. 1997). This suggests that accretion events are very small and very ‘compact’. Smaller MBHs, powering low luminosity AGN, likely grow by accreting smaller packets of material, such as tidally disrupted stars (for MBHs with mass $< 2 \times 10^6 M_\odot$,

Milosavljević et al. 2006), or possibly molecular clouds (Hopkins & Hernquist 2006).

Compact self-gravitating cores of molecular clouds (MC) can occasionally reach subparsec regions. Although the rate of such events is uncertain, we can adopt the estimates of Kharb et al. (2006), and assume that about 10^4 of such events happen within the total activity lifetime of a Seyfert. We can further assume a lognormal distribution (peaked at $\log(M_{\text{MC}}/M_{\odot}) = 4$, with a dispersion of 0.75) for the mass function of MC close to galaxy centers (based on the Milky Way case, e.g., Perets et al. 2007). The result is, on the whole, similar to that produced by minor mergers of black holes (Hughes & Blandford 2003), that is a spin down in a random walk fashion (Volonteri et al. 2007).

In a gas-poor elliptical galaxy, however, substantial populations of molecular clouds are lacking (e.g., Sage et al. 2007), eliminating this channel of MBH feeding. Main sequence stars, however, linger in galaxy centers. Tidal disruption of stars is a feeding mechanism that has been proposed long ago (Hills 1975; Rees 1988). One expects discs formed by stellar debris to form with a random orientation. Stellar disruptions would therefore contribute to the spin-down of MBHs. In an isothermal cusp, assuming that MBH masses scale with the velocity dispersion, σ , of the galaxy (we adopt here the Tremaine et al. 2002 scaling), we can derive the relative mass increase for a MBH in 1 billion years:

$$\frac{M_*}{M_{\text{BH}}} = 0.37 \left(\frac{M_{\text{BH}}}{10^6 M_{\odot}} \right)^{-9/8}. \quad (4)$$

The maximal level of spin down would occur assuming that all the tidal disruption events form counterrotating discs, leading to retrograde accretion. Eq. 4 shows that a small (say $10^5 M_{\odot}$) MBH starting at $a = 0.998$ would be spun down completely, as its mass increase is larger than $\sqrt{3/2}$ (cfr. section 2). On the other hand the spin of a larger (say $10^7 M_{\odot}$) MBH would not be changed drastically. This feeding channel is likely efficient in early type discs which typically host faint bulges characterized by steep cusps, as exemplified above. The situation is different for giant ellipticals: the central density profile displays a shallow core, and tidal disruption of stars is unlikely.

Volonteri et al. (2007) therefore suggest the spin of MBHs in giant elliptical galaxies is likely dominated by massive accretion events which follow gas-rich galaxy mergers (see Dotti et al. in this volume for a discussion of spin evolution in ellipticals formed in gas-poor mergers). Both tidal disruption of stars, and accretion of gaseous clouds is unlikely in shallow, stellar dominated galaxy cores. In a galaxy displaying instead power-law (cuspy) brightness profiles, the rate of stellar tidal disruptions is much higher and random small mass accretion events contribute to spin MBHs down. This result is in agreement with Sikora et al. (2007) who found that disc galaxies tend to be weaker radio sources with respect to elliptical hosts.

Acknowledgments. M.V. acknowledges support from NASA award ATP NNX10AC84G.

References

Berti E., Volonteri M., 2008, ApJ, 684, 822

- Blandford R. D., Netzer H., Woltjer L., Courvoisier T. J.-L., Mayor M., eds, 1990, Physical processes in active galactic nuclei.
- Brenneman L. W., Reynolds C. S., 2006, *ApJ*, 652, 1028
- Campanelli M., Lousto C. O., Zlochower Y., Merritt D., 2007, *Physical Review Letters*, 98, 231102
- Dotti M., Colpi M., Haardt F., 2006, *MNRAS*, 367, 103
- Dotti M., Colpi M., Haardt F., Mayer L., 2007, *MNRAS*, 379, 956
- Dotti M., Ruszkowski M., Paredi L., Colpi M., Volonteri M., Haardt F., 2009, *MNRAS*, 396, 1640
- Dotti M., Volonteri M., Perego A., Colpi M., Ruszkowski M., Haardt F., 2010, *MNRAS*, 402, 682
- Downes D., Solomon P. M., 1998, *ApJ*, 507, 615
- Gammie C. F., Shapiro S. L., McKinney J. C., 2004, *ApJ*, 602, 312
- González J. A., Spherhake U., Brüggemann B., Hannam M., Husa S., 2007, *Physical Review Letters*, 98, 091101
- Herrmann F., Hinder I., Shoemaker D., Laguna P., Matzner R. A., 2007, *ApJ*, 661, 430
- Hills J. G., 1975, *Nat*, 254, 295
- Ho L. C., Filippenko A. V., Sargent W. L. W., 1997, *ApJ*, 487, 591
- Hopkins P. F., Hernquist L., 2006, *ApJS*, 166, 1
- Hughes S. A., Blandford R. D., 2003, *ApJ*, 585, L101
- Kharb P., O’Dea C. P., Baum S. A., Colbert E. J. M., Xu C., 2006, *ApJ*, 652, 177
- King A. R., Pringle J. E., 2006, *MNRAS*, 373, L90
- Körding E. G., Jester S., Fender R., 2006, *MNRAS*, 372, 1366
- Mayer L., Kazantzidis S., Madau P., Colpi M., Quinn T., Wadsley J., 2007, *Science*, 316, 1874
- Mayer L., Kazantzidis S., Mastropietro C., Wadsley J., 2007, *Nat*, 445, 738
- Merloni A., Heinz S., 2008, *MNRAS*, 388, 1011
- Milosavljević M., Merritt D., Ho L. C., 2006, *ApJ*, 652, 120
- Miniutti G., Panessa F., de Rosa A., Fabian A. C., Malizia A., Molina M., Miller J. M., Vaughan S., 2009, *MNRAS*, 398, 255
- Perets H. B., Hopman C., Alexander T., 2007, *ApJ*, 656, 709
- Rees M. J., 1988, *Nat*, 333, 523
- Schmoll S., Miller J. M., Volonteri M., Cackett E., Reynolds C. S., Fabian A. C., Brenneman L. W., Miniutti G., Gallo L. C., 2009, *ApJ*, 703, 2171
- Soltan A., 1982, *MNRAS*, 200, 115
- Spaans M., Silk J., 2000, *ApJ*, 538, 115
- Thorne K. S., 1974, *ApJ*, 191, 507
- Ulvestad J. S., Ho L. C., 2001, *ApJL*, 562, L133
- Volonteri M., Madau P., Quataert E., Rees M. J., 2005, *ApJ*, 620, 69
- Volonteri M., Sikora M., Lasota J.-P., 2007, *ApJ*, 667, 704
- Wilson A. S., Colbert E. J. M., 1995, *ApJ*, 438, 62